Essential role for MFG-E8 as ligand for $\alpha v \beta 5$ integrin in diurnal retinal phagocytosis

Emeline F. Nandrot*, Monika Anand*, Dena Almeida*, Kamran Atabai†, Dean Sheppard†, and Silvia C. Finnemann*‡§

*Dyson Vision Research Institute, Department of Ophthalmology, ‡Department of Cell and Developmental Biology and Department of Physiology and Biophysics, Weill Medical College of Cornell University, New York, NY 10021; and †Lung Biology Center and Department of Medicine, University of California, San Francisco, CA 94143

The integrin receptor $\alpha v \beta 5$ controls two independent forms of interactions of the retinal pigment epithelium (RPE) with adjacent photoreceptor outer segments that are essential for vision. $\alpha v \beta 5$ localizes specifically to apical microvilli of the RPE and contributes to retinal adhesion that maintains RPE contacts with intact outer segments at all times. Additionally, $\alpha v \beta 5$ synchronizes diurnal bursts of RPE phagocytosis that clear photoreceptor outer segment fragments (POS) shed in a circadian rhythm. Dependence of retinal phagocytosis and adhesion on $\alpha v \beta 5$ receptors suggests that the extracellular matrix ensheathing RPE microvilli contains ligands for this integrin. Here we studied mice lacking expression of functional MFG-E8 to test the contribution of this integrin ligand to $\alpha v \beta 5$ functions in the retina. Lack of MFG-E8 only minimally reduced retinal adhesion. In contrast, lack of MFG-E8, like lack of $\alpha v \beta 5$ receptor, eliminated $\alpha v \beta 5$ downstream signaling involving the engulfment receptor MerTK and peak POS phagocytosis, both of which follow light onset in wild-type retina. MFG-E8-deficient RPE in primary culture retained normal epithelial morphology and levels of apical $\alpha v \beta 5$ receptors, but showed impaired binding and engulfment of isolated POS. Soluble or POS-bound recombinant MFG-E8 was sufficient to fully restore phagocytosis by MFG-E8-deficient RPE. Furthermore, MFG-E8 supplementation strongly increased POS binding by wild-type and MerTK-deficient RPE, but did not affect POS binding by RPE lacking $\alpha v \beta 5$. Thus, MFG-E8 stimulates rhythmic POS phagocytosis by ligating apical $\alpha v \beta 5$ receptors of the RPE. These results identify MFG-E8 as the first extracellular ligand in the retina that is essential for diurnal POS phagocytosis.

adhesion | photoreceptors | retinal pigment epithelium | circadian rhythm | outer segment

The phototransduction machinery of retinal rod and cone photoreceptor neurons localizes to their outer segment portions, which face the apical surface of the retinal pigment epithelium (RPE). Interactions of RPE cells with outer segments support photoreceptor function. RPE cells employ apical surface receptors at all times to promote retinal adhesion stabilizing alignment and RPE microvilli interdigitation with outer segments. Once a day, RPE cells use their apical phagocytic receptors and engulfment machinery to respond to circadian shedding of photoreceptor outer segment fragments (POS) with a vigorous burst of POS phagocytosis. Disruption of retinal adhesion in persistent retinal detachment or incomplete POS clearance by the RPE cause outer segment degeneration and photoreceptor apoptosis (1). Thus, intact receptor-mediated interactions of RPE cells with POS are critical to maintaining vision for life.

$\alpha v \beta 5$ integrin is the only integrin family receptor at the apical surface of the RPE in rodent and human retina (2, 3). $\beta 5$ integrin knockout ($\beta 5^{-/-}$) mice show greatly weakened retinal adhesion at all times of day (4). Furthermore, $\beta 5^{-/-}$ retina lacks the daily rhythm of RPE phagocytosis because $\beta 5^{-/-}$ RPE fails to stimulate peak signaling toward the engulfment receptor MerTK after light onset (5). These findings suggest that $\alpha v \beta 5$ receptors

of the RPE independently contribute to both permanent retinal adhesion and diurnal POS phagocytosis.

The contributions of $\alpha v \beta 5$ integrin to RPE–outer segment interactions imply that $\alpha v \beta 5$ receptors recognize ligand proteins in the retina. Although recent work has shown ligands for integrins and MerTK in the interphotoreceptor matrix, their significance for RPE–photoreceptor interactions *in vivo* has thus far been elusive (6, 7).

The secreted glycoprotein milk fat globule–EGF 8 (MFG-E8) can bind to $\alpha v \beta 3$ and $\alpha v \beta 5$ integrins via its RGD motif (8). Furthermore, a discoidin-like domain at the carboxyl terminus of MFG-E8 recognizes phosphatidylserine residues exposed by apoptotic cells (8). Recognition signals of spent POS in the retina remain unknown, but experimental POS particles quantitatively compete with apoptotic cells for binding by $\alpha v \beta 5$ integrin (9). MFG-E8, which localizes to the subretinal space in the retina (6), could thus provide a molecular link between intact or shed outer segments and $\alpha v \beta 5$ receptors of the RPE. Here we explored mutant mice lacking functional MFG-E8 to determine whether MFG-E8 serves as a retinal ligand for $\alpha v \beta 5$ receptors in retinal adhesion and/or RPE phagocytosis. Our results identify MFG-E8 as the primary ligand responsible for stimulating synchronized $\alpha v \beta 5$ receptor signaling and RPE phagocytosis in the retina.

Results

To identify the role of MFG-E8 in the retina, we studied a mutant mouse strain with a specific disruption in the MFG-E8 gene. Because of insertion of a gene trap vector into exon 7, mutant mice do not express wild-type MFG-E8 (10). Instead, their MFG-E8 gene locus encodes a fusion protein consisting of the first 269 amino acids of MFG-E8, followed by the complete β-gal protein. MFG-E8 mutant mice are phenotypically identical to MFG-E8 knockout mice (10–12). Because MFG-E8 mutant mice lack MFG-E8 function, we refer to them here as $\text{MFG}^{-/-}$ mice. Immunoblot analysis of MFG-E8 expression in eyecups containing neural retina and RPE, and of purified RPE tissue, confirmed MFG-E8 protein expression by wild-type ($\text{MFG}^{+/+}$) RPE (Fig. 1 *A* and *B*, +/+). Multiple bands ranging from molecular sizes of 55 to 65 kDa likely represent long and short isoforms of MFG-E8 and differential glycosylation (arrows). Retinal tissue from mice heterozygous for the MFG-E8 mutation continued to express MFG-E8 albeit at reduced levels (Fig.
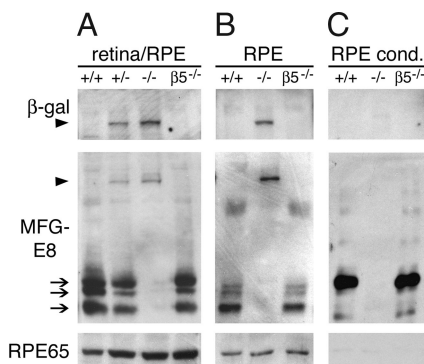
CELL BIOLOGY

Fig. 1. Wild-type but not MFG-E8-mutant RPE cells express and secrete MFG-E8. Lysates prepared from whole eyecups (*A*), purified RPE (*B*), and CM collected from primary RPE cells 1 day after medium change (*C*) were immunoblotted for β-gal, MFG-E8, and the RPE cell marker RPE65 as indicated.
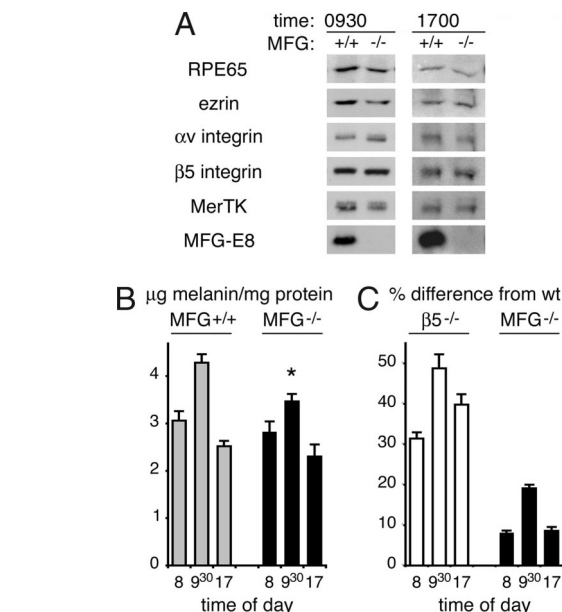

Fig. 2. Retinal adhesion in MFG$^{-/-}$ mice is decreased at the morning peak, but normal at other times. (*A*) Immunoblots of individual MFG$^{+/+}$ and MFG$^{-/-}$ retina samples were probed for RPE proteins as indicated. Only RPE65 at 0930 was decreased by $50 \pm 6\%$ in isolated MFG$^{-/-}$, retina compared with MFG$^{+/+}$ retina (mean $\pm$ SD, $n = 5$; $P < 0.001$; all other proteins, changes $P > 0.05$). (*B*) Quantification of solubilized RPE pigment retrieved with neural retina demonstrated that $19 \pm 1\%$ less pigment fractionated with MFG$^{-/-}$ retina (filled bars) at 0930 than with MFG$^{+/+}$ retina (gray bars) (mean $\pm$ SEM, $n = 12$; *, $P < 0.05$). Samples harvested at 0800 and 1700 contained equal amounts of RPE pigment regardless of MFG-E8 expression (mean $\pm$ SEM, $n = 4$ at 0800; $n = 7$ at 1700; $P > 0.05$). (*C*) Relative RPE pigment retrieval with $\beta5^{-/-}$ (empty bars) and MFG$^{-/-}$ retina (filled bars) was each compared with their respective control strains.

1*A*, $+/-$). As expected, tissues from homozygous MFG$^{-/-}$ littermates expressed no wild-type MFG-E8 (Fig. 1 *A* and *B*, $-/-$). MFG-E8 antibodies used for immunoblotting also recognized a band migrating at the expected molecular size (≈ 200 kDa) of the MFG-E8–β-gal fusion protein in samples of hetero- and homozygous MFG-E8 mutant mice (arrowhead). β-gal immunoblotting of the same samples confirmed that the 200-kDa protein was the MFG-mutant fusion protein (Fig. 1 *A* and *B*, β-gal). Secreted MFG-E8 of ≈ 65 kDa was detected in conditioned medium (CM) of MFG$^{+/+}$, but not of MFG$^{-/-}$ RPE in primary culture (Fig. 1*C*). We found no 200-kDa MFG-fusion protein in CM of MFG$^{-/-}$ RPE. Thus, RPE cells did not secrete the MFG-E8–β-gal fusion protein, but retained it intracellularly like other cell types (10). Immunoblotting for the cytoplasmic RPE-specific protein RPE65 demonstrated a similar load of samples with each tissue type. Lack of RPE65 in CM further indicated that detached or ruptured RPE cells did not contribute to the protein content of these samples. Taken together, these data indicate that RPE cells secrete MFG-E8 and that studying MFG$^{-/-}$ mice allows us to elucidate the function of MFG-E8 in the retina.

Marginally Decreased Retinal Adhesion in Mice Lacking MFG-E8. To compare the strength of retinal adhesion in MFG$^{-/-}$ and wild-type mice, we used a surrogate assay for retinal adhesion, which quantifies RPE pigment and proteins attached to the neural retina after mechanical separation of neural retina from eyecups (4). We tested samples at 0930 and 1700 because these times represent peak and low points of the diurnal variation in retinal adhesion, respectively (4). Fig. 2*A* shows that isolated wild-type and MFG$^{-/-}$ retina contained similar levels of αv, $\beta5$, and MerTK. RPE65, which is exclusive to RPE in the retina, and, to a lower extent, ezrin, which is enriched in RPE apical microvilli, appeared less prominent in MFG$^{-/-}$ samples at 0930, but not at 1700 (Fig. 2*A*). Indeed, compared with wild-type samples, RPE65 in MFG$^{-/-}$ samples was significantly reduced at 0930 (for statistics, see Fig. 2 legend). Ezrin at 0930 and both marker proteins at 1700 did not vary between samples. Quantification of melanin pigment confirmed that retinal adhesion in wild-type mice was stronger than in MFG$^{-/-}$ mice at 0930, but not at 0800 or 1700 (Fig. 2*B*). Subcellular distribution of ezrin, RPE65, and melanin granules was identical in wild-type and MFG$^{-/-}$ RPE at all times of day (data not shown). Taken together, our indirect adhesion assay showed that retinal adhesion in MFG$^{-/-}$ mice was equally strong as retinal adhesion in wild-type mice off-peak, but slightly decreased at the diurnal peak time of adhesion. The same assay demonstrated profound impairment in adhesion at all times of day in $\beta5^{-/-}$ retina

(Fig. 2*C*). Therefore, we concluded that MFG-E8 is not a major ligand for $\alpha v \beta5$ integrin or any other receptor mediating retinal adhesion.

Loss of Daily Phagocytosis Rhythm in Mice Lacking MFG-E8. Next, we determined $\alpha v \beta5$ integrin-dependent phagocytic signaling and uptake in MFG$^{-/-}$ retina. As expected, phosphorylation of the essential engulfment receptor MerTK robustly increased in wild-type retina by 30 min after light onset compared with 1 h before light onset (Fig. 3 *A* and *B*). The same was true for MFG$^{+/-}$ retina. In contrast, MFG$^{-/-}$ retina did not increase MerTK phosphorylation despite normal expression of MerTK and $\alpha v \beta5$. To establish the time course of retinal phagocytosis, we labeled the outer segment protein opsin in retinal cross-sections and surveyed opsin-positive phagosomes in the RPE. Fig. 3 *C* and *D* shows fields representing wild-type and MFG$^{-/-}$ retina at 0630, during the time of peak phagocytosis in wild-type mice. Nuclear staining did not reveal retinal abnormalities in MFG$^{-/-}$ mice (compare red nuclei labeling in Fig. 3 *C* and *D*). Histological staining confirmed normal gross morphology of MFG$^{-/-}$ retinas (data not shown). However, MFG$^{-/-}$ RPE cells contained fewer opsin-positive phagosomes than wild-type RPE (compare green labeling in RPE cell layer in Fig. 3 *C* and *D*; white arrows show examples of individual RPE phagosomes). We then used the same technique to quantify phagosome numbers in retinas obtained at defined times between 0400 and 1400. Fig. 3*E* shows that MFG$^{-/-}$ RPE contained equal numbers of opsin-positive phagosomes at all times of day. Thus, MFG$^{-/-}$ retina lacks the daily rhythm of RPE phagocytosis. In our previous study, we used EM to demonstrate lack of the phago-

Fig. 3. MFG$^{-/-}$ mice lack the synchronized daily activation of MerTK and POS phagocytosis. (A and B) Comparative immunoblotting determined relative phosphorylation levels of MerTK in wild-type MFG$^{+/+}$, MFG$^{-/-}$, and MFG$^{+/-}$ retina. Protein levels of MerTK, β5 integrin, αv integrin, or RPE65 did not vary among samples. Thirty minutes after light onset, MerTK tyrosine phosphorylation was increased by 3.3 ± 0.8-fold and 2.4 ± 0.6-fold in MFG$^{+/+}$ and MFG$^{+/-}$ retina, respectively, compared with 1 h before light onset (mean ± SD, $n = 3$; *, $P < 0.05$). MerTK tyrosine phosphorylation did not significantly change in MFG$^{-/-}$ retina during the same period (1.1 ± 0.8-fold change; $n = 3$; $P > 0.1$). (C and D) (Top) Opsin immunofluorescence (green) of paraffin sections of retinas showed that MFG$^{+/+}$ RPE (C) contained more phagosomes than MFG$^{-/-}$ RPE (D) 30 min after light onset (red, retinal nuclei). Arrowheads show examples of phagosomes. (Middle) Areas marked by white rectangles are enlarged. (Bottom) Conversion of opsin labeling to black and white facilitated counting of opsin-positive phagosomes in the RPE layer. (Scale bars: Upper, 50 μm; Middle, 10 μm.) (E) Phagosome quantification at different times of day demonstrates peak number of phagosomes after light onset in MFG$^{+/+}$ RPE (gray bars) but not in MFG$^{-/-}$ RPE (filled bars) or β5$^{-/-}$ RPE (empty bars; shown previously by EM) (5).

Fig. 4. MFG$^{-/-}$ RPE cells in culture are phenotypically normal, but show impaired POS binding in the absence of exogenous factors. (A–D) Maximal projections of representative fields show similar appearance of double immunofluorescence labeling of adherens junction protein α-catenin (A and B) and β5 integrin (C and D) in primary, unpassaged RPE from MFG$^{+/-}$ (A and C) and MFG$^{-/-}$ (B and D) littermates. (Scale bars: 20 μm.) (E and F) Parallel samples and β5$^{-/-}$ RPE were fed with isolated FITC-POS in DMEM with or without 4% FBS before fixation and quantification of bound (E) and internalized (F) POS. Omitting FBS reduced POS binding by MFG$^{-/-}$ RPE to 47 ± 4% compared with MFG$^{+/-}$ RPE cells ($P < 0.01$, Student's t test). β5$^{-/-}$ POS binding was not significantly altered by FBS ($P > 0.05$). Bars represent mean numbers of bound and internal POS per MFG$^{+/-}$ (gray bars), MFG$^{-/-}$ (filled bars), and β5$^{-/-}$ (light gray bars) RPE cell ± SD ($n = 3$).

cytic peak in β5$^{-/-}$ retina. To directly compare phagosome frequency in MFG$^{-/-}$ and β5$^{-/-}$ retinas, we repeated quantifying phagosome numbers in β5$^{-/-}$ retinas at 1100 and 1400 by counting opsin-positive structures in the RPE. Phagosome densities were identical in β5$^{-/-}$ and MFG$^{-/-}$ RPE, demonstrating

that MFG$^{-/-}$ and β5$^{-/-}$ mice share the same retinal phenotype, a loss of RPE phagocytic rhythm. These data are consistent with a function of MFG-E8 as the sole ligand for αvβ5 integrin in retinal phagocytosis.

Normal Phenotype but Altered POS Binding by MFG$^{-/-}$ RPE Cells. To directly test whether MFG-E8 is relevant for the phagocytic activity of RPE cells, we examined purified, unpassaged RPE cells from MFG$^{-/-}$ mice in primary culture. We isolated MFG$^{-/-}$ RPE with similar yield, viability, attachment, and spreading rates as wild-type RPE (data not shown). Labeling of the adherens junction protein α-catenin showed that MFG$^{+/-}$ and MFG$^{-/-}$ RPE cells in culture had normal epithelial morphology (Fig. 4 A and B). Furthermore, both MFG$^{+/-}$ and MFG$^{-/-}$ RPE expressed αvβ5 integrin at their apical, phagocytic surface (Fig. 4 C and D). When we challenged primary RPE with isolated FITC-labeled POS (FITC-POS), MFG$^{+/-}$ and MFG$^{-/-}$ RPE bound and internalized identical numbers of particles in assay medium containing 4% heat-inactivated FBS (Fig. 4E; 4% FBS). In contrast, MFG$^{-/-}$ RPE bound 48% fewer POS than MFG$^{+/-}$ RPE when we omitted FBS from the assay (Fig. 4E; no FBS). POS binding by β5$^{-/-}$ RPE was low regardless of FBS addition (Fig. 4E). Purified bovine POS used for phagocytosis assays did not contain endogenous MFG-E8 [supporting information (SI) Fig. 6]. It is well established that FBS

promotes engulfment of surface-bound POS by RPE in culture by activating MerTK (13, 14). Hence, lack of FBS practically eliminated POS internalization by all types of RPE tested (Fig. 4F). Taken together, these results indicate that MFG$^{-/-}$ RPE cells in culture have reduced binding activity toward isolated POS in the absence of exogenous factors present in FBS.

Restoration of POS Binding of MFG$^{-/-}$ but Not of β5$^{-/-}$ RPE by Soluble or POS-Bound MFG-E8. To test whether extracellular MFG-E8 could directly promote POS binding by RPE cells, we used the RPE-J cell line, which uses the phagocytic mechanism involving αvβ5 integrin and MerTK to take up POS (15). Fig. 5 A and B illustrates that recombinant MFG-E8 dramatically increased total POS uptake by RPE-J cells (*Upper*). Z scans of the same samples showed that cells receiving MFG-E8 carried more surface-bound POS than control cells (Fig. 5 A and B *Lower*). Quantification of POS uptake confirmed that addition of MFG-E8 was sufficient to robustly increase POS binding and engulfment by FBS-depleted RPE-J cells (Fig. 5 C and D). The effect of MFG-E8 was saturable, and excess levels of MFG-E8 inhibited POS binding and engulfment. These data strongly suggest that the recombinant protein directly participated in POS-RPE binding, rather than activating RPE cells indirectly.

Addition of extracellular recombinant MFG-E8 was sufficient to increase total POS uptake by MFG$^{-/-}$ cells in the absence of FBS (Fig. 5; compare green FITC-POS in E and F). We compared POS binding and internalization in assay medium with and without extracellular MFG-E8 by primary RPE prepared from mice of different genotypes. Like RPE-J cells, wild-type (MFG$^{+/+}$) RPE responded to recombinant MFG-E8 by increasing POS binding (Fig. 5G; MFG$^{+/+}$). Recombinant MFG-E8 was sufficient to restore the reduced POS binding by MFG$^{-/-}$ RPE to the level of POS binding of wild-type RPE (Fig. 5G; MFG$^{-/-}$). Strikingly, recombinant MFG-E8 had no effect on the low levels of POS binding and engulfment by β5$^{-/-}$ RPE cells (Fig. 5G; β5$^{-/-}$). In contrast, Royal College of Surgeons (RCS) rat RPE lacking MerTK dramatically increased POS binding on MFG-E8 addition (Fig. 5G; RCS). POS internalization in the presence of MFG-E8 remained low for all RPE cells tested, which was to be expected during the short time of the uptake assay (Fig. 5G; light bottom part of bars) (5). When we coincubated POS with MFG-E8 or vitronectin in the absence of RPE, we detected both integrin ligands bound to POS by immunoblotting (SI Fig. 7). Such POS-bound MFG-E8 was effective in increasing POS binding by MFG$^{-/-}$ RPE (Fig. 5H; − and +). The activity of POS-bound MFG-E8 did not appear to involve release of MFG-E8 from POS during the assay because adding CM from mock-incubated MFG-E8-POS had no effect (Fig. 5H *Right*). The effect of recombinant-soluble and POS-bound MFG-E8 was specific: Supplementation with neither soluble-purified vitronectin (a known ligand for αvβ5 integrin) nor precoating POS with vitronectin had any effect on POS binding or internalization by wild-type MFG$^{+/+}$ or MFG$^{-/-}$ RPE (SI Fig. 8). Taken together, these data establish that extracellular MFG-E8 plays an essential role in POS phagocytosis. The function of MFG-E8 in POS binding depends on αvβ5 integrin, but is independent of MerTK.

Discussion

This study identifies MFG-E8 as an extracellular ligand protein necessary for rhythmic RPE phagocytosis *in vivo*. Our experiments establish that MFG-E8 promotes the synchronized clearance of spent POS by the RPE in the retina by acting as a ligand for αvβ5 integrin receptors.

Our data analyzing POS phagocytosis in intact retina show that the primary phagocytic and signaling defects of αvβ5 integrin receptor-deficient and MFG-E8 ligand-deficient RPE are identical. Like β5$^{-/-}$ RPE, MFG$^{-/-}$ RPE phagocytoses shed
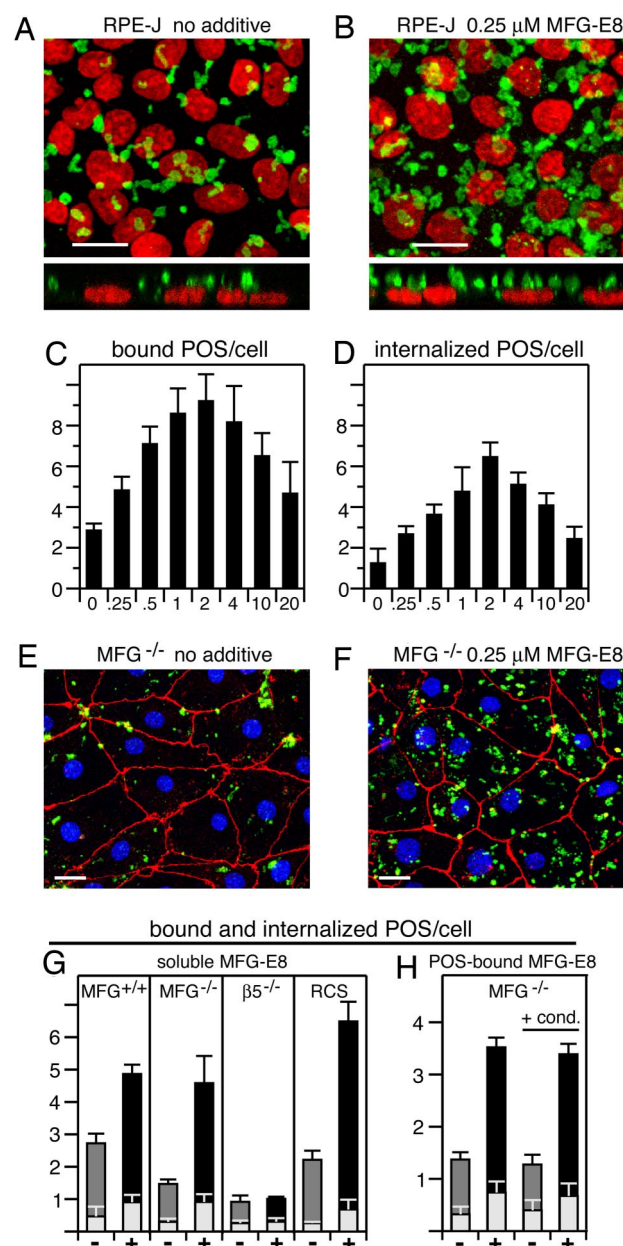

Fig. 5. Recombinant, soluble, or POS-bound MFG-E8 requires αvβ5 integrin to promote POS binding. (A and B) Addition of 0.25 μM MFG-E8 (B) increased total FITC-POS uptake (binding plus engulfment) by RPE-J cells, compared with no additive (A) as seen in maximal projections of x–y confocal stacks (*Upper*) and in single x–z confocal scans (*Lower*). Green, FITC-POS; red, RPE-J nuclei. (Scale bars: 10 μm.) (C–F) Fluorescence quantification showed that soluble MFG-E8 increased POS binding (C) and internalization (D) in a dose-dependent manner. High doses inhibited both phases of uptake. Addition of MFG-E8 increased total POS uptake of primary MFG$^{-/-}$ RPE cells (F), compared with no additive (E). Green, FITC-POS; red, RPE tight junction protein ZO-1; blue, RPE nuclei. (Scale bars: 10 μm.) (G) Fluorescence scanning quantified FITC-POS uptake by RPE as indicated with (+) and without (−) 0.25 μM soluble MFG-E8. MFG-E8 significantly increased POS binding (compare filled top of + bars with dark gray top of − bars) by MFG$^{+/+}$ RPE (mean change 1.8-fold; $P < 0.05$), MFG$^{-/-}$ RPE (3.1-fold; $P < 0.05$), and MerTK-deficient RCS RPE (3.0-fold; $P < 0.05$), but not by β5$^{-/-}$ RPE (1.1-fold; $P > 0.1$). (H) POS-bound recombinant MFG-E8 increased POS binding by MFG$^{-/-}$ RPE (2.7-fold; $P < 0.05$). Addition of CM retrieved from MFG-E8-coated POS after 1 h of mock incubation did not change MFG$^{-/-}$ RPE activity [compare − and + bars (*Left*) with − and + bars (*Right*)]. All bars represent mean ± SD ($n = 3$). Significance was determined comparing values with and without MFG-E8 using Student's t test. POS internalization did not significantly change ($P < 0.05$ for all samples; light bottom parts of bars).

POS, but lacks the diurnal synchronization of POS uptake characteristic of wild-type retina. Our data studying POS phagocytosis by RPE in culture demonstrate that the common phagocytosis phenotype of $\beta5^{-/-}$ and MFG$^{-/-}$ RPE are not coincidental: Soluble or POS-bound extracellular MFG-E8 is required for efficient POS binding to RPE via $\alpha v\beta5$ integrin receptors.

Our data demonstrate that MFG-E8 is an indispensable ligand for $\alpha v\beta5$ function in RPE phagocytosis. In contrast, we found that MFG$^{-/-}$ retinal adhesion differed little from MFG$^{+/+}$ retinal adhesion, a process that also uses $\alpha v\beta5$ receptors. We cannot exclude that compensatory mechanisms may maintain normal strength of retinal adhesion in MFG$^{-/-}$ mice obscuring a function of MFG-E8 in MFG$^{+/+}$ retinal adhesion. However, it is an intriguing possibility that $\alpha v\beta5$ receptors may use an alternate ligand for retinal adhesion that remains to be identified. Notably, vitronectin, a known ligand for $\alpha v\beta5$, has no effect on POS phagocytosis assays. Like this specificity of MFG-E8 for POS phagocytosis, a different $\alpha v\beta5$ ligand may function specifically in retinal adhesion.

The arrhythmic POS clearance by MFG-E8- and $\alpha v\beta5$-deficient RPE implies that MFG-E8 rhythmically activates the $\alpha v\beta5$ integrin signaling pathway involving MerTK in wild-type retina. Thus, either receptor responsiveness and/or ligand availability may vary with time of day and peak concomitant with circadian photoreceptor outer segment shedding. We did not find robust changes of $\alpha v\beta5$ or MFG-E8 protein levels in retina extracts at different times of day. Whole-retina extracts allow us to specifically assess $\alpha v\beta5$ receptors as they relate to photoreceptor–RPE interactions because the primary site of $\alpha v\beta5$ expression in the retina is the apical surface of the RPE (3). In contrast, MFG-E8 localizes to inner and outer rodent retina (6). Therefore, it is possible that whole-retina quantification fails to detect changes in MFG-E8 specifically at the RPE–photoreceptor interface. Better tools to quantify MFG-E8 with sufficient spatial and temporal resolution will be needed to determine whether MFG-E8 levels or subcellular localization change in intact tissue contributing to the precise rhythm of diurnal $\alpha v\beta5$-dependent POS phagocytosis.

Photoreceptor function in $\beta5^{-/-}$ mice progressively declines from 6 months of age (5). The RPE in 12-month-old $\beta5^{-/-}$ mice reveals accumulation of autofluorescent lipofuscin that likely results from inappropriate phagolysosomal digestion (16). These secondary, age-related changes develop by yet unknown mechanisms in $\beta5^{-/-}$ mice. Here we identify mice lacking MFG-E8 ligand as an additional animal model with the same primary defect in RPE phagocytic rhythm as mice lacking $\alpha v\beta5$ receptors. Exploring age-related changes in wild-type, $\beta5^{-/-}$, and MFG$^{-/-}$ mice in parallel may facilitate the future identification of cellular mechanisms that impair RPE and photoreceptor function with age.

Materials and Methods

Reagents. Reagents were from Sigma–Aldrich (St. Louis, MO) unless otherwise stated. Recombinant murine MFG-E8 and laminin were from R&D Systems (Minneapolis, MN). Murine vitronectin was from Molecular Innovations (Southfield, MI).

Animals and Tissue Collection. MFG-E8$^{-/-}$ mice (10) were backbred for three generations to 129T2/SvEmsJ mice (The Jackson Laboratory, Bar Harbor, ME). MFG-E8$^{-/-}$ and control MFG-E8$^{+/+}$ mice from the same generation were used for experiments. $\beta5^{-/-}$ mice, wild-type mice of the same genetic background (129T2/SvEmsJ), and MerTK-deficient RCS-rdy$^{-/-}$-p$^{-/-}$ rats were described previously (5, 15, 17). Mice and rats were housed under cyclic light conditions with lights on at 0600 and off at 1800. Animals were killed by CO_2 asphyxiation. Eyecups were enucleated and processed for microscopy, Western blotting, or RPE isolation as described below. All procedures

involving animals were approved by the Weill Medical College Institutional Animal Care and Use Committee.

In Vivo Retinal Adhesion Assays. Our assay that indirectly assessed adhesion in mouse retina was recently described in detail (4). Briefly, lens and cornea were removed from eyecups immediately postmortem in Hanks saline buffer containing calcium and magnesium. After a radial cut toward the optic nerve, the neural retina was peeled off flattened eyecups. Neural retina samples were lysed in 50 mM Tris·HCl (pH 7.5), 2 mM EDTA, 150 mM NaCl, 1% Triton X-100, 0.1% SDS, and 1% Nonidet P-40 with 1% protease inhibitor mixture. Proteins in cleared supernatants were analyzed by immunoblotting. Melanin pigment of the insoluble pellet after sample lysis was dissolved in 20% DMSO, 2 N NaOH. Samples and commercial melanin standards were quantified measuring absorbance at 490 nm. Pigment was normalized to protein concentration in each sample to account for different tissue yields.

RPE Cell Culture. RPE from 10- to 12-day-old animals was isolated as described (5). Briefly, eyecups were sequentially digested with hyaluronidase and trypsin. Patches of RPE were peeled off Bruch's membrane and seeded on glass coverslips at a density of ≈5 to 10,000 cells per well and grown at 37°C, 10% CO_2 in DMEM with 10% FBS for 4 to 6 days. CM from primary RPE cells were collected after 1 day of culture without serum. The rat RPE-J cell line (ATCC, Manassas, VA) was maintained at 32°C and 5% CO_2 in DMEM with 4% FBS and allowed to polarize for 6 days before use.

Cell and Tissue Lysis and Immunoblotting. Cell and tissue samples were solubilized in 50 mM Hepes (pH 7.4), 150 mM NaCl, 10% glycerol, 1.5 mM $MgCl_2$, and 1% Triton X-100 with 1% each of protease and phosphatase inhibitor cocktails. Protein content of cleared lysates was quantified by using the Bradford colorimetric assay. Whole-cell lysates representing 10,000 RPE cells, 10% of a whole mouse eyecup, or 15% of one isolated mouse retina were separated on 10% SDS-polyacrylamide gels and electroblotted. Immunoblots were probed with primary antibodies to β-gal (Abcam, Cambridge, MA), ezrin (Sigma–Aldrich), αv (BD Bioscience, San Jose, CA) and $\beta5$ integrin (Santa Cruz Biotechnology, Santa Cruz, CA), MerTK and MFG-E8 (R&D Systems), phospho-MerTK (Fabgennix, Frisco, TX), or RPE65 (T. M. Redmond, National Institutes of Health, Bethesda, MD), followed by chemiluminescence detection (PerkinElmer, Waltham, MA). X-ray films were scanned and signals quantified by using NIH ImageJ 1.36b.

Immunofluorescence Microscopy. Eyecups were fixed in formaldehyde/ethanol/acetic acid and embedded in paraffin, then 8-μm cross-sections were cut. Paraffin was removed by using citrus clearing solvent (Richard-Allan Scientific, Kalamazoo, MI). Rehydrated sections were incubated in 5% H_2O_2 in 1× SSC for 10 min to bleach pigment and labeled with rhodopsin antibody B6–30 (P. Hargrave, University of Florida, Gainesville, FL), anti-mouse IgG-AlexaFluor 488 (Invitrogen, Carlsbad, CA), and DAPI, and mounted with Vectashield. Central retinal x–y image stacks were acquired at 0.24-μm intervals on a Leica (Wetzlar, Germany) TSP2 confocal microscope system. Opsin-labeled phagosomes in the RPE were counted on maximal projections of 5-μm-thick stacks. For each data point, we evaluated 12 projections, two each taken from six different eyes, harvested from four different mice. Areas of at least 100 μm of uninterrupted retina/RPE were counted. Phagosome counts were normalized to length of retina and averaged. Significance of difference between wild-type and MFG$^{-/-}$ phagosome count at each time point was determined by using Student's t test.

Cultured cells were fixed in ice-cold methanol and labeled

with antibodies to α-catenin (Sigma–Aldrich) or ZO-1 (Invitrogen). Surface $\alpha v \beta 5$ integrin levels were assessed by live labeling of prechilled cells for 45 min on ice with $\beta 5$ integrin monoclonal antibody before fixation (5). AlexaFluor-conjugated secondary antibodies and DAPI nuclei stain were from Invitrogen. Maximal projections of representative x–y stacks acquired at 0.2-μm intervals on a Leica TSP2 confocal microscopy system were recompiled in Adobe Photoshop 7.0 (Adobe Systems, Mountain View, CA).

***In Vitro* POS Phagocytosis Assays.** POS were isolated from bovine eyes obtained fresh from the slaughterhouse and covalently labeled with FITC dye (Invitrogen) according to established protocols (3). In some assays, recombinant integrin ligand proteins at 1 μM were incubated with FITC-POS in serum-free DMEM on a rotator at 4°C for 1 h to allow binding. Coated FITC-POS were washed three times in excess serum-free DMEM before resuspension at equal particle concentration and use in phagocytosis assays. Binding of recombinant proteins to FITC-POS was assessed by immunoblotting (SI Fig. 7). Confluent RPE cells were preincubated for 30 min in serum-free DMEM before challenge with ≈ 10 FITC-POS per cell in DMEM with or without supplements for the duration of the experiment. Excess POS were removed with three washes in PBS with 1 mM $MgCl_2$, 0.2 mM $CaCl_2$, and cells were lysed or fixed in ice-cold methanol. FITC-POS were quantified as previously described by fluorescence scanning of coverslips mounted on glass slides by using a TYPHOON TRIO scanner and Image-Quant 1.2 (Molecular Dynamics, Sunnyvale, CA) (9). For each condition, at least three independent experiments with triplicate samples were performed and averaged.

1. Cook B, Lewis GP, Fisher SK, Adler R (1995) *Invest Ophthalmol Visual Sci* 36:990–996.
2. Anderson DH, Johnson LV, Hageman GS (1995) *J Comp Neurol* 360:1–16.
3. Finnemann SC, Bonilha VL, Marmorstein AD, Rodriguez-Boulan E (1997) *Proc Natl Acad Sci USA* 94:12932–12937.
4. Nandrot EF, Anand M, Sircar M, Finnemann SC (2006) *Am J Physiol* 290:C1256–C1262.
5. Nandrot EF, Kim Y, Brodie SE, Huang X, Sheppard D, Finnemann SC (2004) *J Exp Med* 200:1539–1545.
6. Burgess BL, Abrams TA, Nagata S, Hall MO (2006) *Mol Vision* 12:1437–1447.
7. Prasad D, Rothlin CV, Burrola P, Burstyn-Cohen T, Lu Q, Garcia de Frutos P, Lemke G (2006) *Mol Cell Neurosci* 33:96–108.
8. Hanayama R, Tanaka M, Miwa K, Shinohara A, Iwamatsu A, Nagata S (2002) *Nature* 417:182–187.
9. Finnemann SC, Rodriguez-Boulan E (1999) *J Exp Med* 190:861–874.
10. Atabai K, Fernandez R, Huang X, Ueki I, Kline A, Li Y, Sadatmansoori S, Smith-Steinhart C, Zhu W, Pytela R, *et al*. (2005) *Mol Biol Cell* 16:5528–5537.
11. Ensslin MA, Shur BD (2003) *Cell* 114:405–417.
12. Hanayama R, Tanaka M, Miwa K, Nagata S (2004) *J Immunol* 172:3876–3882.
13. Mayerson PL, Hall MO (1986) *J Cell Biol* 103:299–308.
14. Finnemann SC, Silverstein RL (2001) *J Exp Med* 194:1289–1298.
15. Finnemann SC (2003) *EMBO J* 22:4143–4154.
16. Rakoczy PE, Zhang D, Robertson T, Barnett NL, Papadimitriou J, Constable IJ, Lai CM (2002) *Am J Pathol* 161:1515–1524.
17. Huang X, Griffiths M, Wu J, Farese RV, Jr, Sheppard D (2000) *Mol Cell Biol* 20:755–759.